applied sciences

MDPI

Article

Mechanistic Interpretation of Ethanol-Pretreatment-Enhanced Drying of Beetroot Through Coupled Diffusion–Shrinkage Modeling

Christos Sarakinou and Athanasia M. Goula *

Department of Food Science and Technology, School of Agriculture, Forestry and Natural Environment, Aristotle University, 541 24 Thessaloniki, Greece; xwerco@gmail.com
* Correspondence: athgou@agro.auth.gr; Tel.: +30-2310-991658

Abstract

Accurate prediction of moisture transfer during drying processes remains challenging. In the present study, a progressive numerical framework was developed to investigate moisture diffusion in ethanol-pretreated beetroot by systematically incorporating increasing levels of physical complexity into Fick's second law of diffusion. Four one-dimensional formulations were examined, including constant moisture diffusivity, shrinkage under constant diffusivity, moisture-dependent effective diffusivity, and a fully coupled model combining moisture-dependent diffusivity with shrinkage. The methodology was further extended to two dimensions to evaluate the spatial evolution of moisture. The governing equations were solved using an implicit Crank–Nicolson finite difference scheme, while shrinkage was introduced through a time-dependent computational domain and moisture-dependent diffusivity was implemented as a variable transport property. The predicted moisture distributions demonstrated that incorporating shrinkage reduced the diffusion path length, whereas moisture-dependent diffusivity provided a more realistic representation of the transport resistance. The coupled formulation produced the most physically consistent description of moisture migration by simultaneously accounting for both mechanisms. Furthermore, the two-dimensional simulations provided additional insight into the spatial redistribution of moisture. The proposed framework establishes a physically based interpretation of the enhanced drying behavior observed after ethanol pretreatment and provides a flexible computational methodology for analyzing moisture transfer.

Keywords: beetroot drying; ethanol pretreatment; moisture diffusivity; shrinkage modeling; finite difference simulation; convective drying

Check for updates

Academic Editor: Andrea Bassani

Received: 17 July 2026
Revised: 17 August 2026
Accepted: 19 August 2026
Published: 20 August 2026

Copyright: © 2026 by the authors. Licensee MDPI, Basel, Switzerland. This article is an open access article distributed under the terms and conditions of the Creative Commons Attribution (CC BY) license.

1. Introduction

Convective drying is one of the most widely applied preservation techniques in the food industry because it effectively reduces water activity, extends shelf life, and facilitates the storage and transportation of agricultural products. Since the pioneering work of Lewis [1], drying has been recognized as a complex transport phenomenon involving simultaneous heat and mass transfer. Comprehensive descriptions of industrial drying technologies and their engineering applications are provided by Crank [2], Mujumdar [3], and Lewicki [4]. Despite its widespread industrial use, convective drying remains a challenging process because the physical properties and geometry of biological materials continuously evolve throughout dehydration.

Among root vegetables, beetroot (*Beta vulgaris* L.) has attracted considerable scientific and industrial interest owing to its high nutritional value and abundance of bioactive

compounds, including betalains, phenolic compounds, vitamins, and dietary fibers. These constituents are associated with antioxidant activity and various health-promoting effects, increasing consumer demand for high-quality dried beetroot products. However, convective drying may adversely affect color, texture, nutritional composition, and overall product quality if the process is not properly controlled. Consequently, significant research has focused on improving drying efficiency while preserving product quality.

Several experimental studies have investigated the drying kinetics and mathematical modelling of beetroot under convective hot-air drying conditions. Gokhale and Lele [5] developed mathematical models describing beetroot drying kinetics, while Ingle et al. [6] evaluated empirical drying models under different operating conditions. More recently, Dasore et al. [7] analyzed thin-layer drying behavior of beetroot, whereas de França et al. [8] combined digital image analysis with near-infrared spectroscopy to monitor drying kinetics and quality evolution. These studies demonstrate that beetroot drying is governed by complex moisture transfer mechanisms that cannot always be adequately represented by simplified empirical correlations.

Pretreatment techniques have been widely investigated as an effective strategy for enhancing drying performance and improving product quality. Among these methods, ethanol pretreatment has received increasing attention because it accelerates moisture removal without requiring substantial modifications to conventional drying equipment. Corrêa et al. [9] first demonstrated that ethanol immersion enhances convective drying of bananas, while Rojas and Augusto [10] provided a detailed mechanistic interpretation of ethanol-assisted drying and its influence on moisture transfer and rehydration behavior. Similar improvements have subsequently been reported for scallion [11] and garlic slices [12], confirming that ethanol pretreatment enhances internal moisture transport in a wide range of plant tissues. For beetroot specifically, Fotiou and Goula [13] experimentally demonstrated that ethanol pretreatment significantly accelerates drying kinetics under various pretreatment conditions, although the underlying transport mechanisms responsible for this enhancement remain insufficiently quantified from a mathematical perspective.

Mathematical modelling has become an essential tool for analyzing moisture transfer during drying and for predicting drying kinetics under different operating conditions. Diffusion-based models derived from Fick's second law [14] have been extensively employed because they provide a physically meaningful description of internal moisture migration while maintaining relatively low computational complexity. Classical analytical solutions proposed by Crank [2] generally assume constant effective moisture diffusivity and fixed sample geometry. Although these assumptions simplify the governing equations, they do not adequately represent the evolving characteristics of biological materials during dehydration.

Experimental and theoretical investigations have shown that moisture transfer is strongly influenced by both structural deformation and variations in effective moisture diffusivity. Mayor and Sereno [15] demonstrated that shrinkage significantly affects heat and mass transfer by continuously modifying the geometry of food materials during drying [16–18]. Similarly, Chen et al. [19] and Srikiatden and Roberts [20] reported that effective moisture diffusivity evolves continuously with moisture content and therefore should be treated as a variable transport property rather than a constant material parameter [21,22]. Neglecting either mechanism may substantially reduce the predictive capability of diffusion models, particularly during the later stages of drying when structural changes become increasingly significant [23,24].

This work addresses this gap by developing a progressive diffusion-based numerical framework for modelling moisture transfer during the convective drying of ethanol-pretreated beetroot. The proposed methodology systematically investigates four one-

dimensional formulations of increasing physical complexity, including constant effective diffusivity, shrinkage under constant diffusivity, moisture-dependent diffusivity, and a fully coupled model incorporating both moisture-dependent diffusivity and geometrical shrinkage. The numerical framework is implemented using an implicit Crank–Nicolson finite difference scheme and is subsequently extended to a two-dimensional formulation to investigate the spatial evolution of moisture within the drying material.

Unlike previous diffusion-based studies that primarily investigate individual transport mechanisms separately, the present work systematically evaluates their individual and combined contributions within a progressive numerical modelling framework. By combining physically based transport mechanisms with experimentally derived relationships for effective moisture diffusivity and shrinkage, the proposed approach provides a comprehensive mathematical interpretation of the enhanced drying behavior produced by ethanol pretreatment while establishing a flexible computational methodology applicable to different food materials, pretreatment techniques, and drying conditions.

2. Materials and Methods

2.1. Sample Preparation and Experimental Drying

Fresh red beetroots (*Beta vulgaris* L., *Detroit* variety) were obtained from a farm in Pella (North Greece), harvested in 2024. Prior to dehydration, the samples were thoroughly washed, peeled, and cut into slices of uniform geometry to ensure consistent drying conditions and minimize experimental variability. Sample dimensions (2 cm cubes) were selected according to the experimental protocol employed in the original drying study [13]. Initial moisture content was 87.66 $\pm$ 0.54% wet basis (w.b.).

Before convective drying, the beetroot samples were subjected to ethanol ($\geq$99.5% purity, food grade, from Sigma-Aldrich (Millipore Sigma, Burlington, MA, USA)) pretreatment. Ethanol solutions of 30–100% v/v were formulated and beetroot cubes were immersed in ethanol solution (solid:liquid ratio 1:8 g/mL) in covered glass beakers kept in a water bath at temperatures of 25–55 °C for pretreatment times of 10–30 min. After pretreatment, excess ethanol was removed from the sample surface before drying. Untreated samples were also considered as reference material for comparison with the ethanol-pretreated samples.

Drying experiments were conducted in a laboratory-scale convective hot-air dryer (Memmert U40, Memmert GmbH + Co. KG, Schwabach, Germany) operating under controlled conditions. Throughout the experiments, the drying air temperature (70 °C) and airflow velocity (1.2 m/s) were maintained constant, while the sample mass was periodically measured using a precision analytical balance (KERN PCB 1000-2, Kern & Sohn GmbH, Balingen, Germany). Drying was continued until the samples reached a moisture content of approximately 15% w.b.

The experimental drying and shrinkage data used for model development and validation were obtained from the experimental investigation previously reported by Fotiou and Goula [13]. That study provides a comprehensive description of the drying protocol, ethanol pretreatment conditions, and experimental methodology, whereas the present work focuses on the development, implementation, and validation of mathematical diffusion models using the published experimental dataset.

The experimental drying curves obtained under these controlled conditions served as the reference dataset for validation of the numerical models developed in this study. Rather than proposing a new experimental drying methodology, the present work focuses on the development of progressively more realistic diffusion models capable of reproducing the experimentally observed moisture evolution. Accordingly, the experimental measurements constitute the benchmark against which the predictive capability of each numerical formulation was systematically evaluated.

2.2. Mathematical Modeling of Moisture Diffusion

Moisture transfer during convective drying was described using Fick's second law of diffusion [2], assuming that internal diffusion represents the dominant mechanism governing moisture migration during the falling-rate drying period. Since no constant drying-rate period was observed experimentally [13], moisture movement within the beetroot samples was modelled as a transient diffusion process.

The dimensionless moisture ratio (MR) was used to describe drying behavior according to [25]:

$$MR = \frac{X - X_e}{X_0 - X_e} \tag{1}$$

where X represents moisture content expressed as percentage wet basis (% w.b.) at time t, X_0 is the initial moisture content, and X_e is the equilibrium moisture content.

The experimental drying rate (DR) was determined from:

$$DR = \frac{m_d \Delta X}{A_s \Delta t} \tag{2}$$

where m_d denotes the dry solid mass, A_s is the exposed drying surface area, and ΔX represents the moisture variation during the time interval Δt.

Assuming isotropic moisture transfer and negligible internal moisture generation, the governing diffusion equation is expressed by Fick's second law:

$$\frac{\partial X(z,t)}{\partial t} = \frac{D_{eff} \partial^2 X(z,t)}{\partial z^2} \tag{3}$$

where D_{eff} is the effective moisture diffusivity and z represents the spatial coordinate.

For constant diffusivity and uniform initial moisture distribution, the analytical solution proposed by Crank [2] was adopted as the reference formulation for comparison with the numerical simulations.

$$MR = \left(\frac{8^3}{\pi^6}\right) \Sigma_{n=1}^{\infty} \left(\frac{1}{(2n-1)^6}\right) \exp\left(-\frac{(2n-1)^2 3\pi^2 D_{eff} t}{4L^2}\right) \tag{4}$$

The numerical solution satisfies the following conditions:

Initial condition:

$$X(z,0) = X_0(z) \tag{5}$$

Symmetry condition:

$$\left(\frac{\partial X}{\partial z}\right)_{z=0} = 0 \tag{6}$$

Surface equilibrium condition:

$$X(L,t) = X_e \tag{7}$$

Although a uniform moisture distribution is often assumed in diffusion studies, the numerical simulations were initialized using a Gaussian-type moisture profile to facilitate visualization of moisture redistribution within the computational domain. Since the primary objective of this work was to compare the behavior of progressive diffusion formulations under identical conditions, the same initial profile was consistently applied in all simulations. The above conditions describe zero moisture flux at the sample center due to symmetry, and equilibrium moisture concentration at the external surface throughout the drying process.

Although the analytical formulation assumes constant transport properties, biological materials continuously undergo structural modifications during drying. Consequently, the proposed modelling framework systematically incorporates moisture-dependent diffusivity and sample shrinkage to improve the physical representation of moisture transport.

2.3. Numerical Solution and Implementation

The governing diffusion equation was solved numerically using the implicit Crank–Nicolson finite difference method because of its second-order accuracy in both space and time and the well-known unconditional stability property of the linear Crank–Nicolson formulation.

The computational domain was discretized using uniformly distributed spatial nodes, whereas time integration was performed using constant time increments. Spatial derivatives were approximated by central finite differences, resulting in a tridiagonal system of algebraic equations solved at each time step.

Initially, a reference model assuming constant effective diffusivity and fixed sample geometry was implemented. Subsequently, increasingly realistic numerical formulations were developed by incorporating sample shrinkage, moisture-dependent diffusivity, and finally the simultaneous coupling of both mechanisms.

Sample shrinkage was introduced through dynamic updating of the computational geometry during drying, whereas the effective moisture diffusivity was recalculated as a function of the local moisture content. These modifications allowed both the transport coefficient and the computational domain to evolve continuously throughout the simulation.

The governing equations were implemented in Python (version 3.10.12) using scientific computing libraries for matrix operations, numerical linear algebra, interpolation, and graphical post-processing. Sparse matrix techniques were employed to improve computational efficiency, while the modular structure of the code enabled each physical mechanism to be activated independently without altering the numerical solution procedure.

Four successive numerical formulations were evaluated: (i) constant diffusivity with fixed geometry, (ii) constant diffusivity including shrinkage, (iii) moisture-dependent diffusivity without shrinkage, (iv) the fully coupled model combining moisture-dependent diffusivity and shrinkage, and (v) a two-dimensional extension of the coupled formulation. This progressive modelling strategy enabled the contribution of each physical mechanism to moisture transport to be systematically evaluated under identical drying conditions. The nonlinear diffusivity term was evaluated using the moisture content obtained from the previous time step. The resulting semi-implicit formulation preserved the tridiagonal structure of the Crank–Nicolson discretization and was solved sequentially at each time step using sparse matrix solvers implemented in Python.

3. Results

3.1. Moisture Diffusion with Constant Diffusivity and Fixed Geometry

The first numerical formulation assumes constant effective moisture diffusivity and fixed sample geometry throughout the drying process. Under these assumptions, moisture migration was governed exclusively by Fick's second law, expressed by Equation (3), while neither the transport coefficient nor the computational domain changed during the simulation.

The spatial field is defined symmetrically in space:

$$-L_z < \mathrm{z} < L_z \tag{8}$$

Effective diffusivity depends on moisture content [13]:

$$D_{eff} = 1.9371 \times 10^{-10} + 8.036 \times 10^{-12}\exp(0.0451 \times X) \tag{9}$$

thus introducing physical nonlinearity into the problem. However, its value changes within the time loop; therefore, it maintains its initial maximum value (constant diffusivity).

The space is divided into N_z = 500 subintervals, with:

$$\Delta z = \frac{2L_z}{N_z} \tag{10}$$

and in total $n_z = N_z + 1$ spatial nodes.

The second derivative is approximated by central differences:

$$\frac{\partial^2 X}{\partial z^2} \approx \frac{X_{i-1} - 2X_i + X_{i+1}}{\Delta z^2} \tag{11}$$

This discretization leads to a tridiagonal system of equations, as each node is only affected by its two neighbors.

Time is differentiated into 52,800 time steps. The factor $a = \frac{D_{eff}\Delta t}{2\Delta z^2}$ corresponds to the Fourier number of the diffusion and results from the semi-indirect scheme Crank–Nicolson.

As illustrated in Figure 1, the initial moisture profile exhibits the expected Gaussian distribution, with the maximum moisture content located at the center of the sample and gradually decreasing towards the boundaries. As drying proceeds, the moisture profiles become progressively flatter, indicating continuous redistribution of moisture from the interior towards the external surfaces. This behavior is characteristic of diffusion-controlled drying and reflects the gradual reduction in concentration gradients responsible for internal moisture transport.

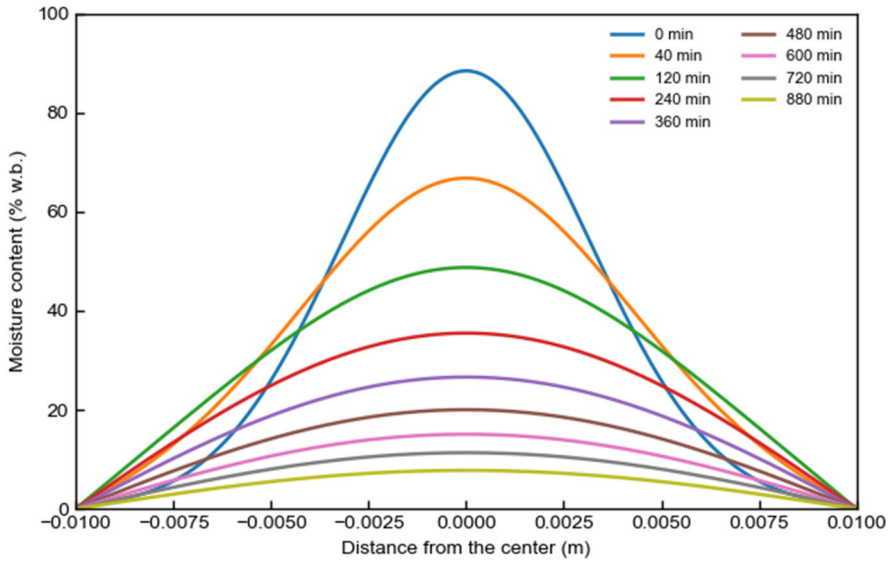


Figure 1. Evolution of the moisture distribution across the sample thickness at different drying times predicted by the one-dimensional diffusion model assuming constant effective moisture diffusivity and fixed geometry.

The progressive decrease in the peak moisture content demonstrates that moisture removal is controlled primarily by internal diffusion during the falling-rate period [25]. Because the effective moisture diffusivity remains constant throughout the simulation, the moisture profiles evolve smoothly and symmetrically, producing a nearly uniform rate of profile relaxation over time. From a mathematical viewpoint, this behavior originates from the gradual decrease in the curvature term $\frac{\partial^2 X}{\partial z^2}$ as the moisture profile flattens. As a direct result, the driving force for diffusion reduces in a gradually uniform manner, regardless of changes in the physical structure of the material.

Although the predicted behavior agrees with the theoretical characteristics of Fickian diffusion, the assumptions adopted in the model inevitably simplify the actual drying process [25]. Biological tissues continuously undergo structural modifications during dehydration, including pore collapse, reduction in internal volume, and changes in transport pathways. Since these mechanisms are neglected in the present formulation, the model represents an idealized description of moisture migration rather than a complete representation of the physical process.

The behavior observed in Figure 1 is consistent with previous diffusion-based studies reporting that constant-property models adequately reproduce the general characteristics of moisture transport during the early stages of drying but gradually lose predictive capability as structural changes become increasingly important [3,6,7].

Therefore, the constant-diffusivity formulation provides an appropriate reference model against which the influence of additional physical mechanisms can be evaluated. In the following section, the computational framework is extended by incorporating sample shrinkage while maintaining constant effective diffusivity, allowing the isolated contribution of geometrical changes to moisture transport to be investigated.

3.2. Effect of Shrinkage Under Constant Diffusivity

The second numerical formulation investigated the influence of sample shrinkage on moisture transport while maintaining a constant effective moisture diffusivity. In this approach, the computational geometry was updated continuously throughout the drying process according to the experimentally determined dimensional changes in the beetroot slices, whereas the diffusion coefficient remained unchanged. This modification allows the numerical model to account for the reduction in the diffusion path length associated with structural deformation during dehydration.

Shrinkage was introduced through a time dependent characteristic length $L(t)$, defining a shrinking spatial domain:

$$z \in [-L(t), L(t)] \tag{12}$$

After coordinate transformation ($\xi = \frac{z}{L(t)}$), the governing equation becomes:

$$\frac{\partial X}{\partial t} = D_{\text{eff}} \frac{1}{L(t)^2} \frac{\partial^2 X}{\partial \xi^2} \tag{13}$$

The factor $1/L(t)^2$ mathematically amplifies the diffusion term as shrinkage proceeds. This mechanism reduces the effective diffusion path, resulting in accelerated moisture removal relative to the fixed geometry situation. Shrinkage does not alter the material's diffusive properties, but it scales the diffusion operator geometrically. Thus, the observed increase in drying rate occurs strictly from spatial compression rather than higher mass transport capability.

As shown in Figure 2, incorporating shrinkage significantly altered the evolution of the internal moisture profiles. Compared with the constant-geometry model, the moisture gradients decreased more rapidly as drying progressed, reflecting the shorter diffusion distances resulting from the progressive reduction in sample thickness. Consequently, moisture migrated more efficiently from the interior towards the external surfaces, producing moisture distributions that evolved at a faster rate than those predicted by the reference model [26].

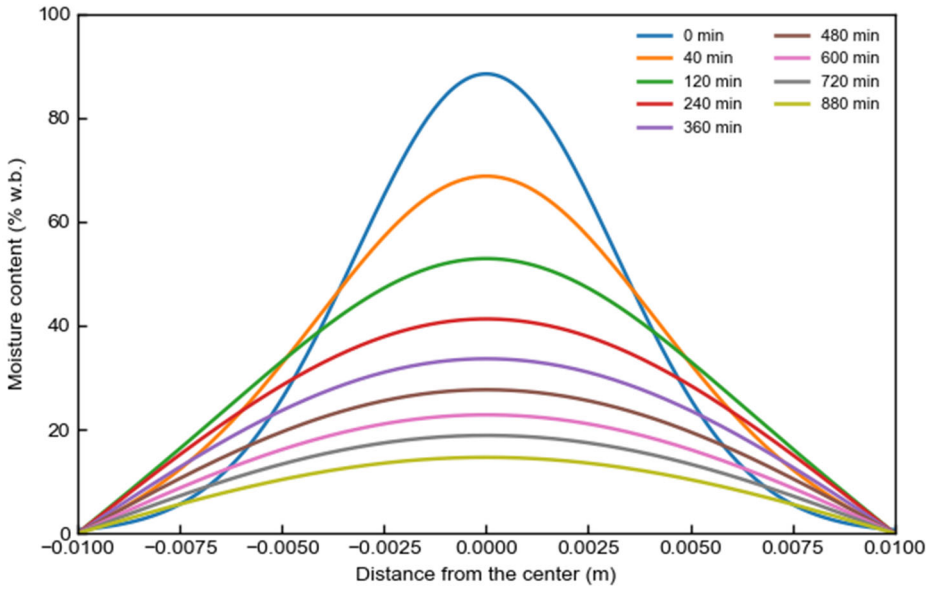


Figure 2. Evolution of the moisture distribution across the sample thickness at different drying times predicted by the one-dimensional diffusion model incorporating sample shrinkage while assuming constant effective moisture diffusivity.

The effect of shrinkage became increasingly pronounced during the intermediate and final stages of drying. At high moisture contents, the geometrical changes were relatively limited, and the predicted profiles remained similar to those obtained using the fixed-geometry formulation [16–18]. As dehydration continued, however, the reduction in sample dimensions accelerated the diffusion process by decreasing the characteristic transport length. This behavior is consistent with the physical expectation that moisture requires increasingly shorter distances to reach the product surface as shrinkage develops.

The improved agreement obtained after incorporating shrinkage highlights the importance of structural deformation during convective drying of biological materials. Ignoring volume reduction results in an overestimation of the diffusion path and consequently underestimates the rate of moisture removal during the later stages of drying [26]. By continuously updating the computational domain, the present formulation provides a more realistic representation of the evolving internal geometry of the beetroot tissue.

Despite this improvement, the numerical predictions still exhibited deviations from experimental observations. These discrepancies indicate that geometrical changes alone cannot fully explain the drying behavior. While shrinkage modifies the distance over which moisture diffuses, the transport coefficient itself is still assumed to remain constant throughout the entire process. The effective moisture diffusivity changes continuously as moisture content decreases and the internal structure of the material evolves.

The influence of shrinkage observed in the present study agrees with previous investigations demonstrating that structural deformation plays a significant role in determining drying kinetics. Mayor and Sereno [6] reported that shrinkage affects both heat and mass transfer by modifying the geometry of the material during dehydration. Similar conclusions have been reported for diffusion-based drying models of fruits and vegetables, where incorporating shrinkage considerably improves agreement between numerical predictions and experimental measurements [26].

Although the inclusion of shrinkage enhanced the physical realism of the numerical model, the remaining discrepancies suggest that accurate prediction of moisture transport also requires consideration of variable transport properties. Consequently, the following section investigates the influence of moisture-dependent effective diffusivity while

maintaining a fixed computational geometry, allowing the individual contribution of the transport coefficient to be evaluated independently of structural deformation.

3.3. Moisture-Dependent Effective Diffusivity Without Shrinkage

The third numerical formulation investigated the influence of moisture-dependent effective diffusivity while maintaining a fixed sample geometry throughout the drying process. Unlike the previous models, the effective moisture diffusivity was continuously updated according to the local moisture content, allowing the transport coefficient to evolve dynamically during dehydration. This approach provides a more realistic representation of internal moisture transport by accounting for the progressive changes in the physical properties of the material as drying proceeds [21,22].

To account for physical changes in the material, the effective diffusivity was expressed as an explicit function of local moisture.

The governing diffusion equation then becomes:

$$\frac{\partial X}{\partial t} = \frac{\partial}{\partial z}\left[D_{eff}(X)\frac{\partial X}{\partial z}\right] \tag{14}$$

Equation (14) is nonlinear, leading to fundamentally different system dynamics. Regions with high moisture content present higher diffusivity, advancing fast early-stage moisture redistribution.

Figure 3 illustrates the incorporation of moisture-dependent diffusivity significantly modified the predicted moisture profiles compared with the constant-diffusivity formulation. The moisture gradients evolved more realistically throughout the drying process, particularly during the intermediate and final drying stages, where the influence of decreasing moisture content on internal transport became increasingly important. The simulated profiles exhibited a smoother transition between successive drying times, reflecting the continuous adaptation of the transport coefficient to the local moisture conditions.

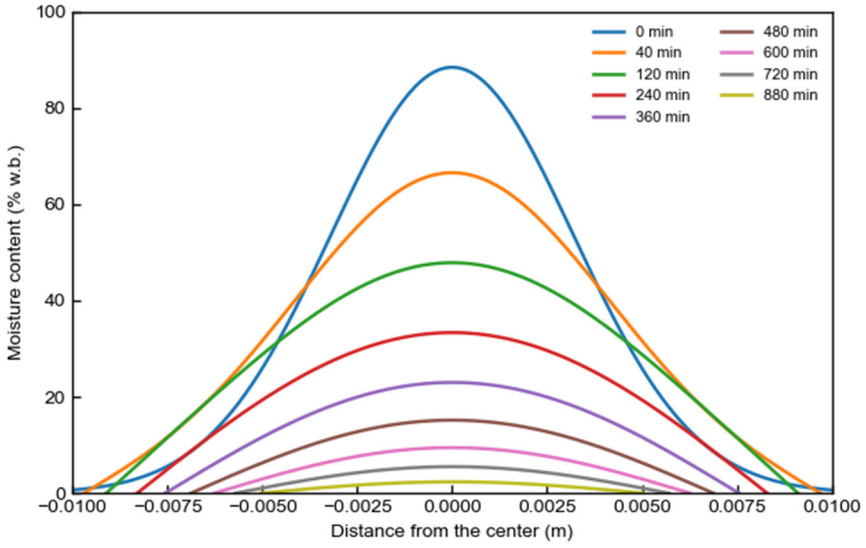


Figure 3. Evolution of the moisture distribution across the sample thickness at different drying times predicted by the one-dimensional diffusion model assuming moisture-dependent effective diffusivity without considering sample shrinkage.

The improved behavior of the model is attributed to the direct relationship between moisture content and effective diffusivity. As dehydration progresses, the internal structure of the beetroot tissue undergoes gradual modifications that affect pore connectivity, cellular integrity, and moisture mobility. Representing diffusivity as a variable property enables

these changes to be incorporated into the governing equation, resulting in a more accurate description of moisture migration than that obtained using a single constant diffusion coefficient [22].

Compared with the shrinkage model presented in the previous section, the present formulation produced a more substantial improvement in the predicted moisture evolution. This observation suggests that the evolution of transport properties has a stronger influence on moisture redistribution than geometrical changes alone. While shrinkage modifies the effective diffusion distance, moisture-dependent diffusivity directly affects the governing transport mechanism by continuously adjusting the resistance to moisture movement within the material [26].

Nevertheless, some discrepancies between the numerical predictions and the experimental observations remained evident, particularly towards the end of the drying process. Although the transport coefficient evolved continuously with moisture content, the computational domain remained fixed throughout the simulation. Consequently, the model did not account for the progressive reduction in sample dimensions accompanying dehydration. The absence of structural deformation therefore limited the overall predictive capability of the numerical formulation.

These findings are consistent with previous studies reporting that effective moisture diffusivity should be considered a variable material property rather than a constant parameter during food drying. Chen et al. [7] demonstrated that moisture-dependent diffusivity substantially improves the prediction of drying kinetics, while Srikiatden and Roberts [8] reported similar observations for biological materials exhibiting significant structural evolution during dehydration. Such studies support the conclusion that realistic modelling of moisture transport requires continuous updating of the transport properties throughout the drying process.

Overall, the results demonstrate that incorporating moisture-dependent effective diffusivity provides a considerable improvement over the constant-diffusivity formulation and enhances the physical realism of the numerical model. However, accurate prediction of drying behavior still requires simultaneous consideration of structural deformation. For this reason, the following section presents the fully coupled numerical model, in which both moisture-dependent diffusivity and sample shrinkage are incorporated within a unified computational framework.

3.4. Fully Coupled Model: Moisture-Dependent Diffusivity and Shrinkage

The fourth numerical formulation combined the two principal mechanisms governing moisture transport during convective drying, namely moisture-dependent effective diffusivity and geometrical shrinkage. Unlike the previous models, both the transport coefficient and the computational domain evolved simultaneously throughout the simulation, allowing the numerical framework to account for the continuous interaction between material properties and structural deformation.

The formulation combines moisture dependent diffusivity with shrinkage:

$$\frac{\partial X}{\partial t} = \frac{1}{L(t)^2}\frac{\partial}{\partial \xi}\left[D_{eff}(X)\frac{\partial X}{\partial \xi}\right] \tag{15}$$

This equation includes two independent nonlinearities: property nonlinearity through $D_{eff}(X)$ and geometric nonlinearity through $L(t)$. Early drying stages are governed by high diffusivity at higher moisture levels, whereas intermediate stages present competing effects between geometric compression and declining diffusivity. At later stages, moisture transport becomes almost exclusively controlled by the low $D_{eff}(X)$ plateau.

As shown in Figure 4, the fully coupled formulation produced the smoothest evolution of the internal moisture profiles during drying. The predicted moisture distributions exhibited a gradual reduction in concentration gradients while simultaneously reflecting the progressive decrease in sample thickness. This behavior is consistent with the expected physical response of biological materials, where moisture migration is controlled by continuously changing transport properties within an evolving geometry.

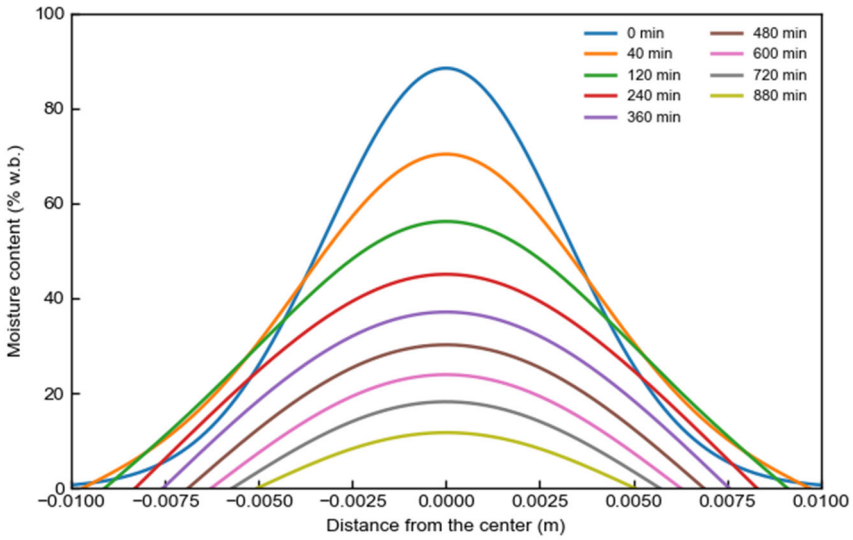


Figure 4. Evolution of the moisture distribution across the sample thickness at different drying times predicted by the fully coupled one-dimensional model incorporating both moisture-dependent effective diffusivity and sample shrinkage.

Compared with the previous numerical formulations, the coupled model provided a more realistic description of moisture redistribution throughout the drying process. During the early drying stages, when moisture content remained relatively high and structural changes were limited, the predicted profiles were comparable to those obtained using the simpler formulations. However, as dehydration progressed, the simultaneous evolution of effective diffusivity and sample dimensions became increasingly important, allowing the model to reproduce the changing internal moisture gradients more consistently.

These findings demonstrate that neither geometrical shrinkage nor moisture-dependent diffusivity alone is sufficient to fully describe moisture transport in dehydrating beetroot tissue. Shrinkage reduces the characteristic diffusion length by continuously modifying the computational domain, whereas variable diffusivity reflects the progressive changes in the resistance to internal moisture migration [16–18]. Since both mechanisms develop simultaneously during drying, their combined implementation provides a more physically consistent representation of the dehydration process than either assumption considered independently.

The coupled formulation also demonstrates the advantages of adopting a progressive modelling strategy. Starting from the reference diffusion model and sequentially incorporating individual physical mechanisms enabled the contribution of each modelling assumption to be evaluated within the same numerical framework. This approach facilitates the interpretation of the drying process while avoiding the introduction of unnecessary model complexity at the initial stages of the analysis.

The behavior observed in Figure 4 is consistent with previous studies emphasizing that accurate prediction of drying kinetics requires simultaneous consideration of variable transport properties and structural changes. Mayor and Sereno [6] highlighted the importance of shrinkage in modifying heat and mass transfer during dehydration, while Chen

et al. [7] and Srikiatden and Roberts [8] demonstrated that effective moisture diffusivity should be treated as a variable property rather than a constant material parameter. The present results support these observations by integrating both mechanisms into a unified numerical formulation and demonstrating their complementary roles in moisture transport.

An important feature of the proposed model is its flexibility. Because both shrinkage and moisture-dependent diffusivity are incorporated within the same finite difference framework, additional physical mechanisms may be included without modifying the overall numerical solution strategy. This modular structure facilitates future applications of the model to different food materials, drying conditions, or pretreatment techniques through appropriate adjustment of the governing transport relationships.

Overall, the fully coupled model represents the most comprehensive formulation investigated in this work. By simultaneously accounting for evolving material properties and structural deformation, it provides the most physically realistic description of moisture migration among the examined one-dimensional models. This formulation therefore serves as the basis for the two-dimensional simulations presented in the following section, where the spatial distribution of moisture within the entire sample is investigated.

3.5. Two-Dimensional Generalization and Spatial Consistency

The final stage of the numerical investigation consisted of extending the fully coupled one-dimensional formulation to a two-dimensional computational domain. This extension enabled the spatial evolution of moisture within the entire beetroot slice to be examined, providing additional insight into the internal redistribution of moisture during drying. The same physical assumptions adopted in the coupled one-dimensional model were retained, including moisture-dependent effective diffusivity and time-dependent sample shrinkage.

The two-dimensional governing equation is written as:

$$\frac{\partial X}{\partial t} = \nabla \cdot \left[D_{eff}(X) \nabla X \right] \tag{16}$$

As illustrated in Figure 5, the two-dimensional simulations reveal the development of non-uniform moisture distributions throughout the drying process. At the beginning of drying, the moisture field remained relatively homogeneous, reflecting the nearly uniform initial moisture content of the sample. As dehydration progressed, increasingly steep moisture gradients developed near the exposed boundaries, while the central region retained higher moisture levels for a longer period. This behavior demonstrates the gradual migration of moisture from the interior towards the drying surfaces.

The numerical solution preserves spatial symmetry and stability, demonstrating that the Crank–Nicolson scheme accurately represents the nonlinear diffusion operator without introducing artificial anisotropy. The predicted moisture contours remained smooth and physically consistent throughout the simulation, indicating numerical stability of the finite difference implementation. No artificial oscillations or discontinuities were observed in the calculated moisture field, confirming that the implicit Crank–Nicolson scheme [2] successfully handled the coupled effects of variable diffusivity and continuously evolving geometry.

Agreement between one- and two-dimensional solutions proves that the observed trends are inherent to the governing equations, not artifacts of dimensional reduction. Compared with the one-dimensional formulation, the two-dimensional model provided a more comprehensive representation of moisture transport by accounting for moisture migration in both spatial directions. While the one-dimensional approach adequately describes drying in thin samples where transport is predominantly normal to the surface,

the two-dimensional formulation captures lateral moisture redistribution that may become significant in samples with finite width or non-uniform geometries.

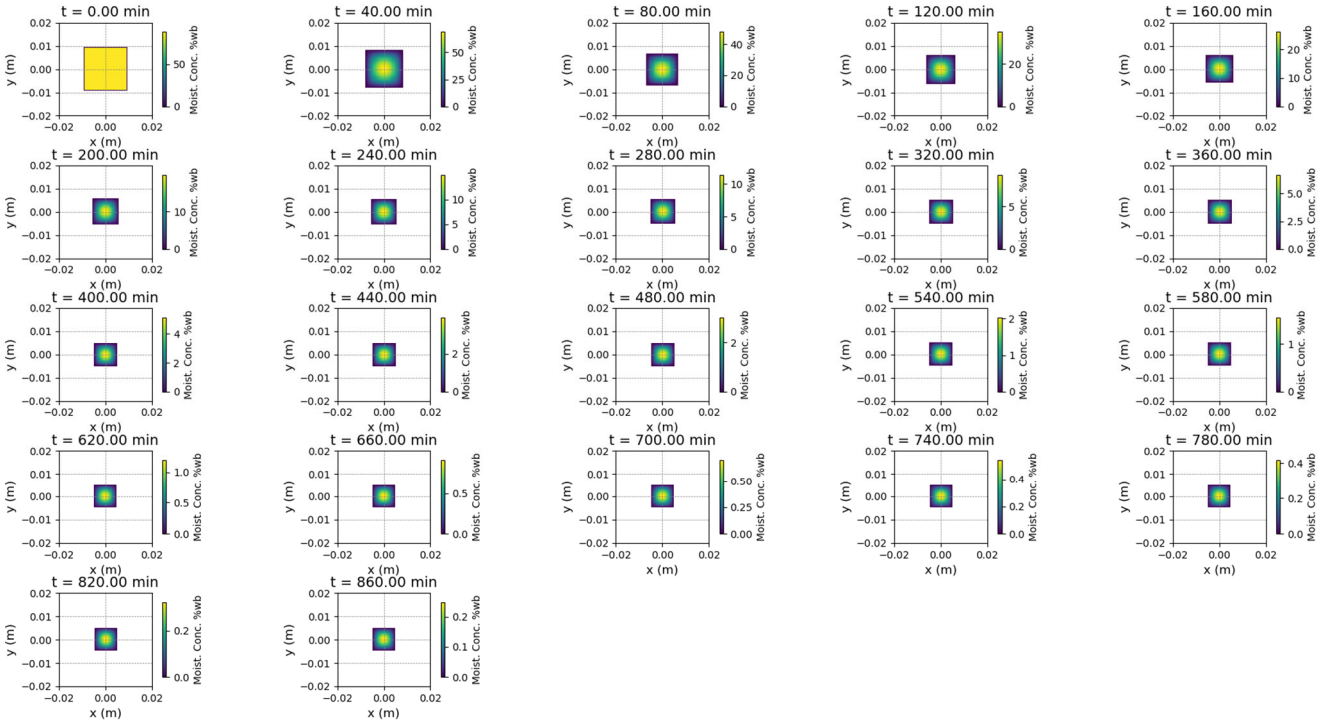


Figure 5. Two-dimensional moisture distribution predicted by the fully coupled diffusion model at representative drying times.

The two-dimensional simulations also provide a useful visualization of the progressive reduction in moisture gradients during dehydration. As drying proceeds, the moisture field becomes increasingly uniform owing to the combined effects of internal diffusion, decreasing moisture content and geometrical shrinkage. This behavior agrees with the expected physical evolution of diffusion-controlled drying and supports the validity of the proposed numerical framework.

Although the present experimental measurements consisted primarily of average moisture values, the two-dimensional model offers information that cannot be obtained directly from conventional drying experiments. In particular, the predicted spatial moisture distributions provide valuable insight into the internal moisture gradients responsible for the observed drying kinetics, thereby improving the physical interpretation of the dehydration process.

The capability to simulate two-dimensional moisture transport also increases the flexibility of the proposed methodology. The numerical framework can readily be adapted to more complex product geometries, different boundary conditions, or heterogeneous material properties without fundamental modifications to the governing numerical algorithm. Such flexibility makes the model suitable for future investigations involving irregular food geometries or alternative drying technologies.

Overall, the two-dimensional extension confirms the robustness and consistency of the coupled numerical formulation [25]. By preserving the physical behavior observed in the one-dimensional simulations while providing additional spatial information, the model establishes a comprehensive framework for analyzing moisture transport during convective drying.

To facilitate a systematic comparison of the proposed numerical formulations, Table 1 summarizes the progressive evolution of the modelling framework in terms of its under-

lying physical assumptions and modelling complexity. Each formulation introduces an additional transport mechanism while preserving the same numerical solution strategy, thereby enabling the individual contributions of shrinkage, moisture-dependent diffusivity, and multidimensional transport to be evaluated independently before their combined implementation. This progressive development establishes the foundation for the mechanistic interpretation of ethanol pretreatment presented in the following section.

Table 1. Progressive evolution of the proposed numerical framework and its physical assumptions.

Numerical Formulation	Diffusivity Representation	Geometry Representation	Primary Physical Contribution	Spatial Domain	Physical Realism
Constant Diffusivity Model	Constant	Fixed geometry	Reference Fickian diffusion	1D	Baseline
Shrinkage-Corrected Model	Constant	Shrinking geometry	Introduction of geometricalevolution	1D	Intermediate
Variable Diffusivity Model	Moisture-dependent	Fixed geometry	Introduction of moisture-dependent transport	1D	Intermediate
Fully Coupled 1D Model	Moisture-dependent	Shrinking geometry	Simultaneous interaction between both mechanisms	1D	Advanced
Fully Coupled 2D Model	Moisture-dependent	Shrinking geometry	Captures two-dimensional moisture redistribution	2D	Most comprehensive

3.6. Mathematical Interpretation of Ethanol Pretreatment

The proposed numerical framework provides a physically meaningful interpretation of the influence of ethanol pretreatment on convective drying. Rather than modifying the governing diffusion equation, ethanol pretreatment is interpreted as affecting the transport parameters controlling internal moisture migration. Consequently, the drying enhancement observed experimentally can be represented mathematically through the simultaneous evolution of the effective moisture diffusivity and the characteristic diffusion length.

Ethanol pretreatment is mathematically represented via increased diffusivity parameters:

$$D_{\text{eff, eth}}(X) > D_{\text{eff, control}}(X) \tag{17}$$

Therefore:

$$\nabla \cdot [D_{\text{eth}}(X)\nabla X] > \nabla \cdot [D_{\text{control}}(X)\nabla X] \tag{18}$$

The acceleration of drying occurs directly from an improved diffusion operator, not from phenomenological fitting. This formulation couples microstructural modification induced by ethanol with macroscopic transfer improvement in a fully mechanistic manner.

The influence of these two mechanisms is evident from the progressive comparison of the numerical models presented in Figures 1–5. Models employing constant effective diffusivity or fixed geometry successfully reproduce the general drying trend but cannot fully capture the experimentally observed moisture redistribution. Incorporating moisture-dependent diffusivity improves the description of the changing transport properties, whereas inclusion of shrinkage accounts for the continuously decreasing diffusion distance. The fully coupled model, combining both mechanisms, produces the most realistic prediction of the internal moisture field and the temporal evolution of moisture gradients.

Figures 6 and 7 present the results obtained from the mathematical solution for two different pretreatment conditions, whereas Figure 8 presents a comparison of the predictions for each experimental condition.

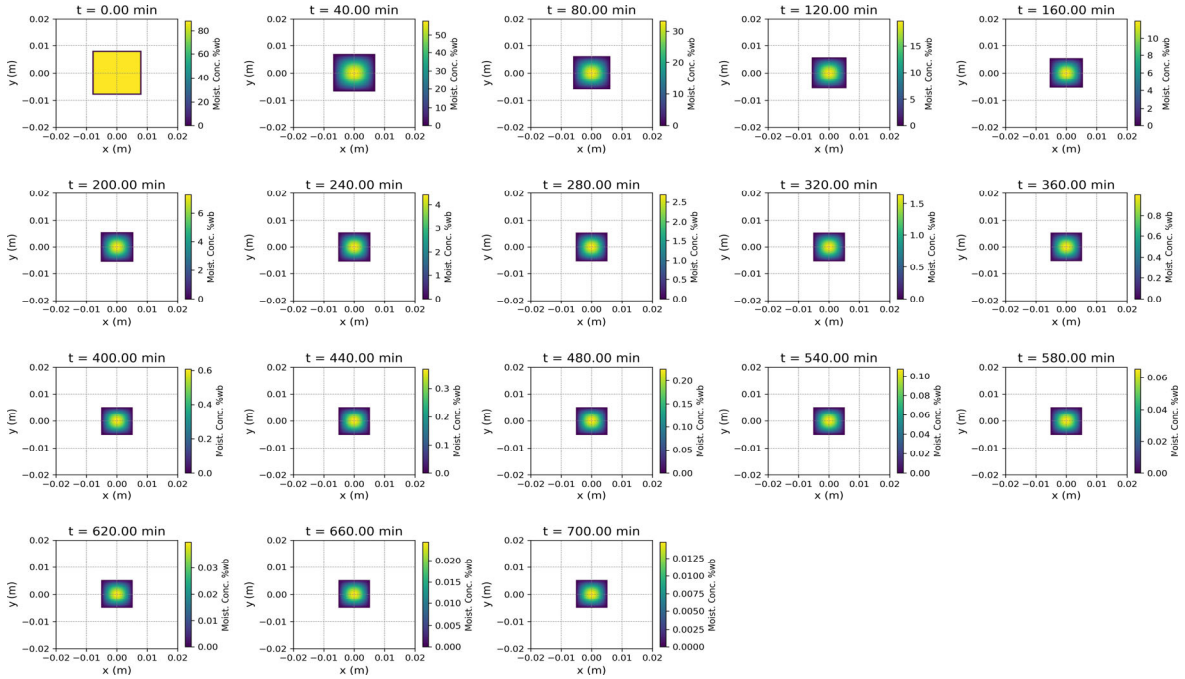


Figure 6. Evolution of moisture content (% wet basis) in the two-dimensional spatial grid for various time points during drying after ethanol pretreatment at 40 °C for 20 min with ethanol concentration of 100%.

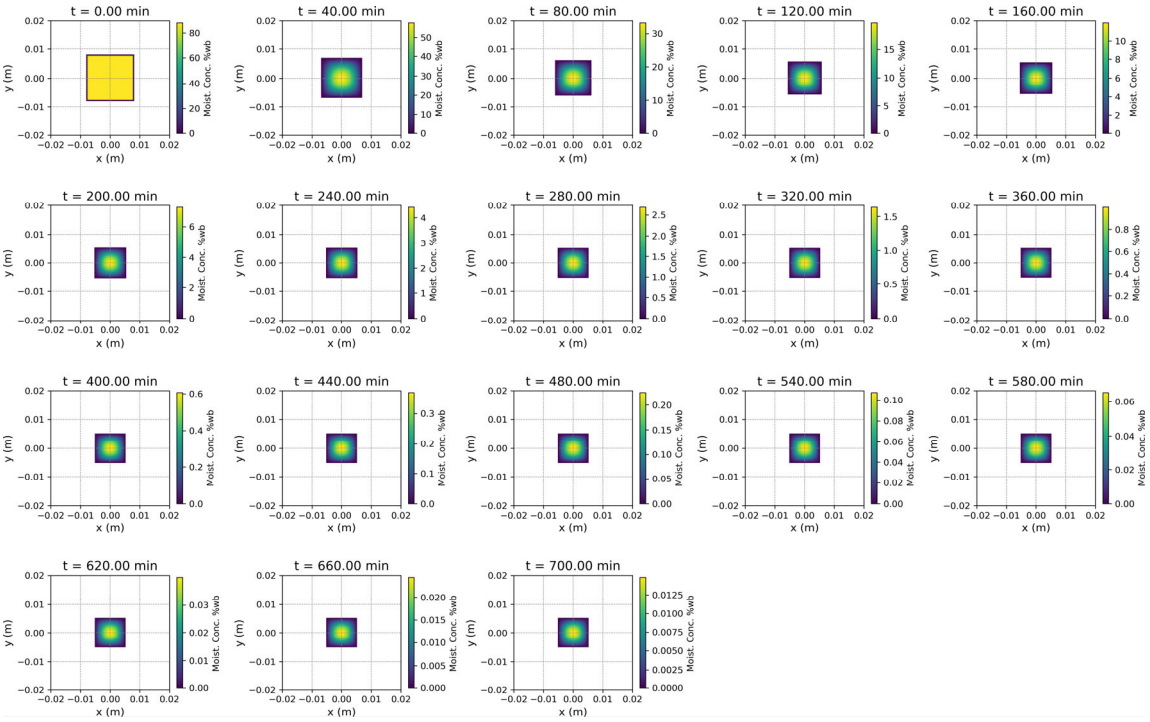


Figure 7. Evolution of moisture content (% wet basis) in the two-dimensional spatial grid for various time points during drying after ethanol pretreatment at 55 °C for 20 min with ethanol concentration of 65%.

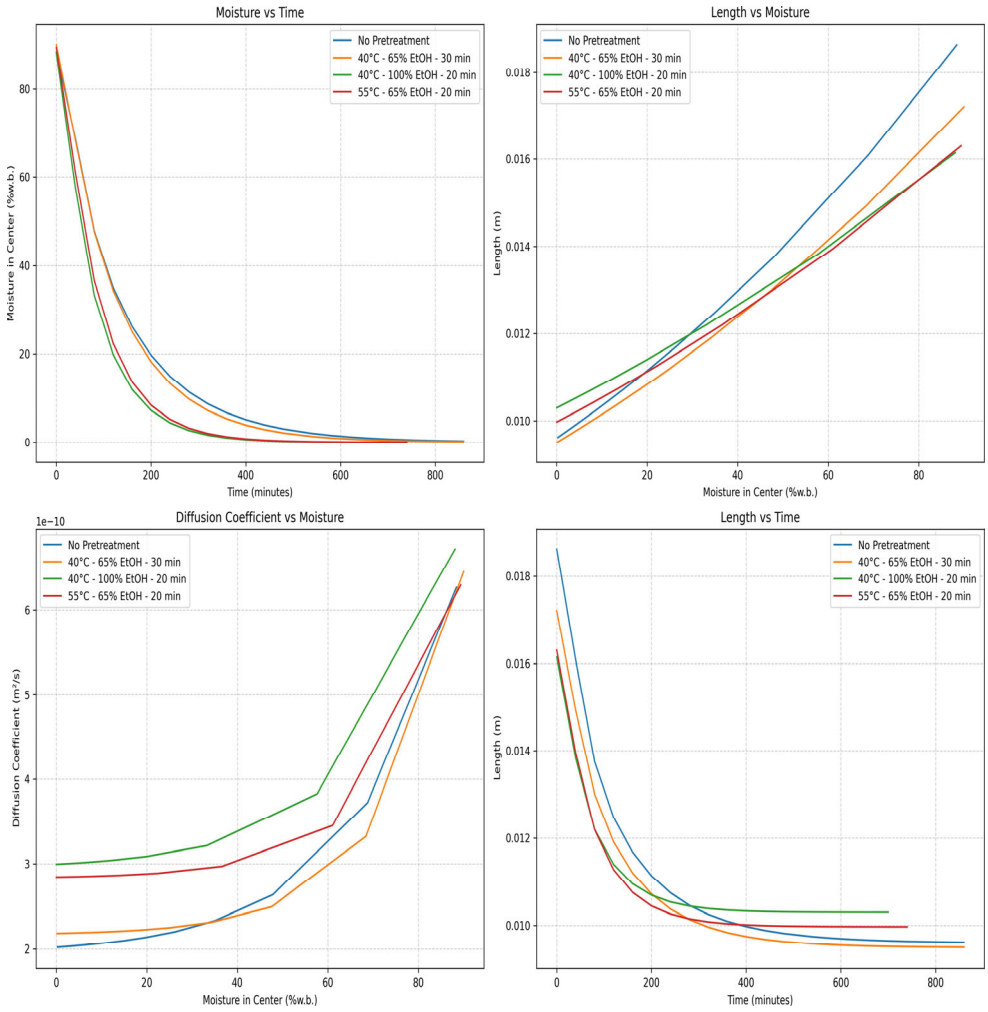


Figure 8. Predictions of moisture, dimensional and diffusion coefficient changes for three different pretreatment conditions.

The comparison of the simulations clearly shows the effect of ethanol pretreatment on the changes in moisture, length, and diffusion coefficient compared to the simulation without pretreatment. The simulations with pretreatment show variations depending on the parameters: temperature, ethanol concentration and pretreatment time. Specifically, higher temperatures or higher ethanol concentrations tend to accelerate the moisture reduction and increase diffusion, resulting in the sample shrinking faster and the moisture in the center decreasing earlier compared to the non-pretreated sample [10–13].

The simulation without pretreatment shows a slower evolution of the phenomena and constitutes essentially the reference point, allowing the evaluation of the effectiveness of ethanol [27]. The differences observed between the simulations with different pretreatment conditions highlight the importance of optimizing the parameters (temperature, concentration, time) to maximize the drying speed or the treatment efficiency.

Overall, the results confirm that ethanol pretreatment significantly affects the drying kinetics and spatial distribution of moisture [9–11]. The simulation provides a comprehensive picture of how variable pretreatment conditions modify the diffusion and changes in the sample length, while the comparison with the non-pretreated sample makes clear the necessity of optimizing the parameters for desired results.

Before examining in detail the effect of pretreatment and its different conditions on drying, it is important to compare the simulation results with the corresponding experimental data. As shown in Figure 9:

1. Effect of pretreatment: Ethanol pretreatment has a clear effect on the drying dynamics. Pretreated samples show a faster moisture reduction compared to the non-pretreated case, confirming the overall effectiveness of the treatment. In addition, pretreatment improves the uniformity of diffusion, allowing the samples to reach a steady state of moisture more quickly.
2. Effect of pretreatment conditions: Different pretreatment conditions—temperature, ethanol concentration and time—affect moisture reduction and length change differently. Higher temperatures or higher ethanol concentrations accelerate the drying process, while increased pretreatment time further enhances the effect. The combinations of parameters create variations in the spatial distribution of moisture and sample shrinkage, highlighting the importance of optimizing conditions for desired results.
3. Comparison with experimental values: The comparison of the simulations with the experimental data shows similar trends between numerical predictions and experimental observations for moisture and length change. Small deviations are observed at extreme times or in areas with abrupt changes, where the experimental measurements may be affected by local anomalies. The comparison confirms that the simulation provides a physically consistent representation of the observed drying behavior and allows the evaluation of the effect of different pretreatment conditions. The simulation shows that the optimizations of the drying by ethanol pretreatment, such as changing the temperature, concentration or time, generally reproduce the overall evolution observed experimentally. The simulation predictions for moisture reduction and sample length change reflect the actual measurements, confirming that the modeling can be reliably used to evaluate the effectiveness of pretreatment and select optimal drying conditions. The agreement between simulation and experiments highlights the potential of using the model to adapt and optimize drying processes in practical applications. Although the present study focused primarily on the mechanistic interpretation of moisture transport and the comparative evaluation of progressive diffusion formulations, future work should include a comprehensive quantitative validation using statistical performance indicators such as *RMSE*, *MAE*, and R^2 to further assess predictive accuracy under different drying conditions.

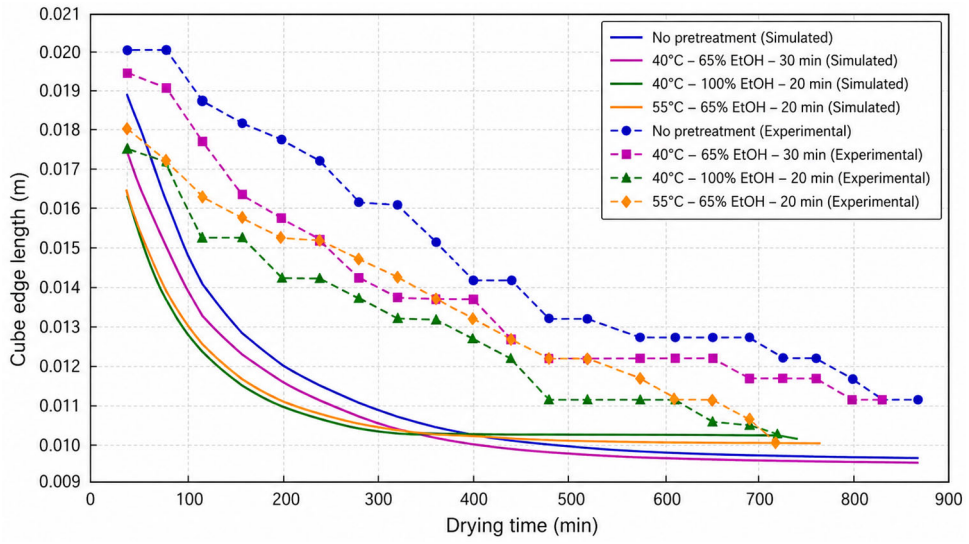


Figure 9. Comparison between numerical predictions and experimental measurements of cube edge length during convective drying of untreated and ethanol-pretreated beetroot samples. Experimental points were obtained from Fotiou and Goula [13], while solid lines represent predictions of the present numerical model.

4. Discussion

The application of ethanol pretreatment at a specific temperature and for a specific time substantially affects the drying kinetics of beetroot, reducing the total moisture removal time compared to the sample without pretreatment. The increase in pretreatment temperature and the presence of ethanol lead to an enhancement of mass transfer, which is attributed to the partial degradation of the cell walls, the reduction in capillary forces and the replacement of part of the free water by ethanol. Pretreatment conditions at 55 °C with 65% ethanol show the fastest kinetics, while the use of 100% ethanol at 40 °C accelerates mainly the initial stage of drying.

The spatial distribution of moisture, as derived from the simulation, confirms that the drying is mainly controlled by internal diffusion mechanisms. In all cases, a faster moisture reduction is observed in the areas near the sample surface and a slower removal in the center, resulting in the development of sharp moisture gradients in the initial stages of the process. The presence of pretreatment reduces these gradients, leading to a more uniform moisture distribution during drying, which indicates an increase in the effective diffusion coefficient [27].

The comparison of simulated and experimental results shows a systematic deviation, with the experimental data showing a slower decrease in the average moisture content, especially in the initial and middle stages. This deviation is largely explained by the fact that in the experiment, time zero corresponds to the entry of the sample, at ambient temperature, into the drying oven. Consequently, part of the initial time is spent heating the material until conditions favorable for intense moisture diffusion are achieved. In contrast, in the simulation, diffusion starts instantaneously at time zero, an assumption that leads to an overestimation of the initial drying rate.

Furthermore, the inherent non-uniformity of the experimental tests, both in terms of the structure of the plant material and the initial moisture conditions and thickness of the samples, should be considered. The experimental curves represent average values, which incorporate fluctuations that cannot be fully captured in a deterministic model. Nevertheless, the simulation was based on diffusion coefficients and shrinkage equations derived from the processing of experimental data, which enhances the physical consistency of the model and justifies the overall good qualitative agreement between theory and experiment.

It should be noted that the shrinking-domain formulation adopted in the present work represents a simplified moving-boundary approach, where shrinkage is incorporated through the evolution of the characteristic diffusion length. Although this treatment captures the primary geometrical effect of shrinkage on the diffusion path, additional advection-type terms associated with domain motion were not included explicitly. Consequently, the model should be interpreted as a simplified mechanistic framework rather than a fully rigorous moving-boundary formulation. Future work should address the complete mass-conservative governing equations.

The numerical simulation developed in the context of this work constitutes a deterministic model, in which the evolution of moisture in time and space is fully determined by the diffusion equations, the initial and boundary conditions and the system parameters. For given values of the diffusion coefficient, shrinkage ratios and initial moisture distribution, the model yields a unique and fully repeatable solution, without considering random fluctuations or microstructural non-uniformities of the plant tissue. On the contrary, the experimental results incorporate the inherent non-uniformity of the samples, as well as small deviations in the initial conditions and physical properties of the material, which leads to a dispersion of the measurements. Consequently, the deviations observed between simulated and experimental curves do not necessarily indicate a failure of the model, but reflect the comparison of an idealized, average description of the process with a real process

characterized by natural variability. The simulation, therefore, consistently captures the general trends and dominant mechanisms of drying, while the experimental deviations can be attributed mainly to the inherent inhomogeneity of the material and not to fundamental weaknesses of the numerical approach.

From a theoretical point of view, the drying kinetics is adequately described by a model based on Fick's second law, with a dominant phase of decreasing drying rate, characteristic for plant materials with high internal resistance to mass transfer. The absence of a clear period of constant rate suggests that internal diffusion is the limiting mechanism throughout most of the process [21,22]. Pretreatment changes the effective value of the diffusion coefficient and the shrinkage conditions, shifting the moisture curves towards shorter times without altering the basic form of the kinetics [27].

Overall, the results confirm that diffusion models, when fed with parameters derived from experimental data, can describe with satisfactory accuracy the relative effect of different pretreatment conditions on drying. The observed deviations are mainly attributed to transient heating phenomena and experimental non-uniformity and not to fundamental weaknesses of the model. Consequently, the combined use of experimental investigation and simulation constitutes a reliable tool for the design and optimization of drying processes of plant products.

5. Conclusions

A progressive diffusion-based numerical framework was developed to investigate moisture transport during the convective drying of ethanol-pretreated beetroot. The proposed methodology systematically incorporated constant effective moisture diffusivity, sample shrinkage, moisture-dependent diffusivity, a fully coupled formulation, and a two-dimensional numerical extension. The results demonstrated that incorporating both shrinkage and moisture-dependent effective diffusivity significantly improves the physical representation of moisture migration compared with the classical constant-diffusivity model. The coupled formulation provided the most physically consistent description of the drying process by simultaneously accounting for the evolution of transport properties and structural deformation during dehydration. The two-dimensional extension further demonstrated the capability of the proposed methodology to describe the spatial evolution of moisture within the material, while the mathematical interpretation of ethanol pretreatment established a direct relationship between the experimentally observed enhancement of drying and the underlying transport mechanisms incorporated into the model. Overall, the proposed modelling framework provides a physically based and computationally flexible approach for analyzing moisture transport during convective drying. The methodology can be adapted to different food materials and drying conditions through appropriate modification of the governing transport parameters, providing a useful tool for studying drying kinetics and supporting the optimization of industrial dehydration processes. Future work should focus on extending the proposed framework by incorporating additional transport phenomena that occur during food dehydration, including temperature-dependent effective moisture diffusivity, simultaneous heat and mass transfer, and anisotropic transport properties. The implementation of three-dimensional geometries and validation against local moisture distribution measurements would further improve the predictive capability of the model. From an industrial perspective, the proposed model may assist in identifying operating conditions that maximize moisture removal while minimizing drying time and energy consumption. By predicting the influence of pretreatment intensity on moisture diffusivity and shrinkage behavior, the framework could support optimization of large-scale convective drying operations and facilitate process design for improved product quality and production efficiency.

Author Contributions: Conceptualization, A.M.G.; methodology, C.S.; software, C.S.; validation, C.S.; formal analysis, C.S.; investigation, C.S.; resources, A.M.G.; data curation, C.S. and A.M.G.; writing—original draft preparation, C.S.; writing—review and editing, A.M.G.; visualization, A.M.G.; supervision, A.M.G.; project administration, A.M.G.; funding acquisition, A.M.G. All authors have read and agreed to the published version of the manuscript.

Funding: This research received no external funding.

Institutional Review Board Statement: Not applicable.

Informed Consent Statement: Not applicable.

Data Availability Statement: The datasets used and/or analyzed during the current study are available from the corresponding author on reasonable request.

Conflicts of Interest: The authors declare no conflicts of interest.

Abbreviations

The following abbreviations are used in this manuscript:

A_s	Exposed drying surface area
a	Fourier number parameter of the Crank–Nicolson scheme
D_{eff}	Effective moisture diffusivity
DR	Drying rate
t	Drying time
L	Characteristic diffusion length
$L(t)$	Time-dependent characteristic length during shrinkage
MR	Moisture ratio
m_d	Dry solid mass
N_z	Subintervals
n_z	Spatial nodes
w.b.	Wet basis
X	Moisture content at time t
X_0	Initial moisture content
X_e	Equilibrium moisture content
z	Spatial coordinate
ξ	Dimensionless transformed coordinate
Δt	Time increment
Δz	Spatial increment
$\frac{\partial}{\partial t}$	Time derivative
$\frac{\partial^2}{\partial z^2}$	Second spatial derivative
∇	Gradient operator

References

1. Lewis, W.K. The Rate of Drying of Solid Materials. *J. Ind. Eng. Chem.* **1921**, *13*, 427–432. [CrossRef]
2. Crank, J. *The Mathematics of Diffusion*, 2nd ed.; Oxford University Press: Oxford, UK, 1979.
3. Mujumdar, A.S. *Handbook of Industrial Drying*, 4th ed.; CRC Press: Boca Raton, FL, USA, 2020.
4. Lewicki, P.P. Design of Hot Air Drying for Better Foods. *Trends Food Sci. Technol.* **2006**, *17*, 153–163. [CrossRef]
5. Gokhale, S.V.; Lele, S.S. Dehydration of Red Beet Root (*Beta vulgaris*) by Hot Air Drying: Process Optimization and Mathematical Modeling. *Food Sci. Biotechnol.* **2011**, *20*, 955–964. [CrossRef]
6. Ingle, M.; Nawkar, R.; Godse, S. Drying Kinetics and Mathematical Modeling of Beetroot. *Int. J. Curr. Microbiol. Appl. Sci.* **2019**, *8*, 1926–1934. [CrossRef]
7. Dasore, A.; Polavarapu, T.; Konijeti, R.; Puppala, N. Convective Hot Air Drying Kinetics of Red Beetroot in Thin Layers. *Front. Heat Mass Transf.* **2020**, *14*, 23. [CrossRef]
8. De França, P.R.; Cruz-Tirado, J.P.; Barbin, D.F.; Kurozawa, L.E. Hot Air Drying of Red Beet: Process and Product Quality Monitoring by Digital Images and Near Infrared Spectroscopy. *Dry. Technol.* **2023**, *41*, 1085–1095. [CrossRef]

9. Corrêa, J.L.G.; Braga, A.M.P.; Hochheim, M.; Silva, M.A. The Influence of Ethanol on the Convective Drying of Unripe, Ripe, and Overripe Bananas. *Dry. Technol.* **2012**, *30*, 817–826. [CrossRef]
10. Rojas, M.L.; Augusto, P.E.D. Ethanol Pre-Treatment Improves Vegetable Drying and Rehydration: Kinetics, Mechanisms and Impact on Viscoelastic Properties. *J. Food Eng.* **2018**, *233*, 17–27. [CrossRef]
11. Wang, X.; Feng, Y.; Zhou, C.; Sun, Y.; Wu, B.; Yagoub, A.E.A.; Aboagarib, E.A. Effect of Vacuum and Ethanol Pretreatment on Infrared-Hot Air Drying of Scallion (*Allium fistulosum*). *Food Chem.* **2019**, *295*, 432–440. [CrossRef] [PubMed]
12. Feng, Y.; Zhou, C.; Yagoub, A.E.A.; Sun, Y.; Owusu-Ansah, P.; Yu, X.; Wang, X.; Xu, X.; Zhang, J.; Ren, Z. Improvement of the Catalytic Infrared Drying Process and Quality Characteristics of Dried Garlic Slices by Ultrasound-Assisted Alcohol Pretreatment. *LWT* **2019**, *116*, 108577. [CrossRef]
13. Fotiou, D.; Goula, A.M. Ethanol Pretreatment before Air Drying of Beetroot: Drying Kinetics. *Food Sci. Biotechnol.* **2025**, *34*, 3909–3925. [CrossRef] [PubMed]
14. Fick, A. Ueber Diffusion. *Ann. Phys.* **1855**, *170*, 59–86. [CrossRef]
15. Mayor, L.; Sereno, A.M. Modelling Shrinkage during Convective Drying of Food Materials: A Review. *J. Food Eng.* **2004**, *61*, 373–386. [CrossRef]
16. Cavion, C.; Tonet, J.; Miola, L.D.S.; Perottoni, C.A.; Zorzi, J.E. A heuristic approach to the automated analysis of drying curves. *Int. J. Appl. Ceram. Technol.* **2019**, *16*, 400–403. [CrossRef]
17. Gulati, T.; Datta, A.K. Mechanistic understanding of case-hardening and texture development during drying of food materials. *J. Food Eng.* **2015**, *166*, 119–138. [CrossRef]
18. Nguyen, T.K.; Mondor, M.; Ratti, C. Shrinkage of cellular food during air drying. *J. Food Eng.* **2018**, *230*, 8–17. [CrossRef]
19. Chen, D.; Zheng, Y.; Zhu, X. Determination of Effective Moisture Diffusivity and Drying Kinetics for Poplar Sawdust by Thermogravimetric Analysis under Isothermal Condition. *Bioresour. Technol.* **2012**, *107*, 451–455. [CrossRef] [PubMed]
20. Srikiatden, J.; Roberts, J.S. Measuring Moisture Diffusivity of Potato and Carrot (Core and Cortex) during Convective Hot-Air and Isothermal Drying. *J. Food Eng.* **2006**, *74*, 143–152. [CrossRef]
21. da Silva, W.P.; de Lima, A.G.B.; Pereira, J.C.A.; Gomes, J.P.; Queiroz, A.J.D.M.; de Figueirêdo, R.M.F.; Paiva, Y.F.; dos Santos, F.S.; de Melo, B.A.; Moura, H.V.; et al. A diffusion model to describe water absorption by red rice during soaking: Variable mass diffusivity, variable volume, use of Boundary-Fitted Coordinates. *Processes* **2024**, *12*, 1696. [CrossRef]
22. Goula, A.M.; Thymiatis, K.; Kaderides, K. Valorization of grape pomace: Drying behavior and ultrasound extraction of phenolics. *Food Bioprod. Process.* **2016**, *100*, 132–144. [CrossRef]
23. Wijerathne, A.D.H.T.; Joardder, M.U.H.; Welsh, Z.G.; Nayak, R.; Sablani, S.S.; Karim, A. Recent Advances in Food Drying Modeling: Empirical to Multiscale Physics-Informed Neural Networks. *Compr. Rev. Food Sci. Food Saf.* **2025**, *24*, e70194. [CrossRef] [PubMed]
24. Lončar, B.; Pezo, L. Mathematical Modeling Approach and Simulation in Food Drying Applications. *Foods* **2024**, *13*, 384. [CrossRef] [PubMed]
25. Arpaci, E.; Atayılmaz, Ş.Ö.; Gemici, Z. Exploring Mathematical Modeling and CFD in Convective Drying of Fruits and Vegetables: A Review. *Food Bioprocess Technol.* **2025**, *18*, 3195–3222. [CrossRef]
26. Moradi, M.; Raeesi, R.; Rashidi, S.; Keramat-Jahromi, M. Predictive modeling of apple slice drying: Integrating temperature, thickness, and shrinkage dynamics. *PLoS ONE* **2026**, *21*, e0341428. [CrossRef] [PubMed]
27. Kaveh, M.; Sharifian, F.; Khalife, E.; Keramat, S.; Ghaysari, B.; Dolatkhoh, M.; Jadidi, F. Effect of combined ethanol and ultrasound pretreatment on energy consumption and bioactive compounds of rose petals in hot air drying. *Sci. Rep.* **2025**, *15*, 31327. [CrossRef] [PubMed]

Disclaimer/Publisher's Note: The statements, opinions and data contained in all publications are solely those of the individual author(s) and contributor(s) and not of MDPI and/or the editor(s). MDPI and/or the editor(s) disclaim responsibility for any injury to people or property resulting from any ideas, methods, instructions or products referred to in the content.